WALAILAK JOURNAL
http://wjst.wu.ac.th Engineering and Physical Sciences

Numerical Study of Thermal Behaviors in Roof Ponds Under the Hot and Humid Climate

Sasicha SAKDAWATTANANON[1], Sudaporn SUDPRASERT[1,*] and Phadungsak RATTANADECHO[2]

[1]Faculty of Architecture and Planning (Building Technology), Thammasat University, Pathum Thani 12120, Thailand
[2]Center of Excellence in Electromagnetic Energy Utilization in Engineering (CEEE), Department of Mechanical Engineering, Thammasat University, Pathum Thani 12120, Thailand

([*]Corresponding author's e-mail: sudaporn@ap.tu.ac.th)

Received: 25 September 2015, Revised: 8 May 2016, Accepted: 16 June 2016

Abstract

The passive cooling of building roofs by use of a water roof pond has been of interest for many years, but the thermal behavior of roof ponds lacks detailed analysis leading to high water depths and inaccurate thermal performance estimations. In this study, the effects of solar radiation, ambient temperature, and constant water evaporation on the thermal behavior in roof ponds with depths of 0.1, 0.2, 0.3 and 0.4 m in 2 roof pond patterns; uncovered with and without water flow, were numerically investigated. The numerical results illustrated temperature gradients in the roof pond systems during exposure to a solar intensity of 638 W/m^2, and ambient temperatures of 32.93 - 36.67 °C with an initial water temperature of 24.0 - 25.35 °C. In the uncovered roof pond, the water depth of 0.2 m was found to completely prevent heat transfer into the building. The roof pond with a water flow of 0.1 - 0.4 m removes heat away from the roof through water circulation; hence, the suggestion is to use it in combination with a conventional uncovered roof pond as a hybrid-system. The results reveal important information regarding the complex interaction between temperature distribution in water with mixed convection in the roof-pond in a hot and humid climate.

Keywords: Roof pond, passive system, evaporative cooling, energy efficiency, mixed convection

Nomenclature

c_p	heat capacity, J/kg°C	u	velocity in the x-direction, m/s
d	water depth, m	u_o	initial velocity in the x-direction, m/s
e	evaporative heat loss (W/m^2)	v	velocity in the y-direction, m/s
G	solar intensity, W/m^2	v_{wind}	wind speed, m/s
g	gravitational acceleration (m/s^2)	v_{inlet}	inlet velocity, m/s
h	outdoor convective heat transfer coefficient, W/m^{2}K	β	volume expansion coefficient (1/K)
h_e	evaporative heat transfer coefficient, W/m^{2}Pa	ε_c	emissivity
k	thermal conductivity, W/m°C	η	dynamic viscosity, kg/ms
L	roof pond length, m	ρ	density, kg/m^3

n	outward normal vector to the surface	σ	Stefan-Boltzmann constant of 5.67×10^{-8} W/m^{2}K^4
P	pressure, Pa	υ	viscosity, m^2/s
P_a	water vapor partial pressure at the air temperature, Pa		
P_w	water vapor partial pressure at the water temperature, Pa		**Subscripts**
P_o	atmospheric pressure, Pa	c	concrete
t	time, sec	w	water
T	room air temperature , °C	$\alpha1$	outdoor air
T_0	reference temperature, °C	$\alpha2$	indoor air
T_{sky}	sky temperature, K		
T_w	water temperature, °C		**Superscripts**
$T_{w,\,in}$	inlet water temperature, °C	T	transpose matrix
$T_{w,\,out}$	outlet water temperature, °C		

Introduction

Global warming affects the increase of cooling load in residential buildings and a sustainable solution is needed to reduce cooling energy requirements. Research results found the average surface temperature in the city of Bangkok has increased from 26.01 °C in 1994 to 39.79 °C in 2009 [1] due to the heat island and climate change. In the past, Thai people lived by rivers and ponds and these played important roles in reducing heat and enhancing ventilation with cool air through the house. Presently, urban houses have limited areas, therefore passive cooling strategies such as indirect evaporative cooling and thermal delay using roof ponds is a viable solution for sustainable residential design. With a relative humidity of 46 - 70 percent at a dry-bulb temperature of 33.4 - 37.5 °C during 12.00 - 16.00 h in June - July, indirect evaporative cooling has high potential to partially substitute the mechanical cooling requirement given that it can reduce air temperature by 2.0 - 6.2 °C [2]. The thermal performance of a roof pond system depends on roof pond types, water depths and weather conditions. High thermal performance was found in a roof pond with pond cover in the daytime to prevent direct solar gain and water spray at night time to let heat radiate into the sky [3]. However, this system requires a mechanism to operate the covers and still water would easily become contaminated, as reviewed in Spannaki [3]. On the other hand, the uncovered roof pond exhibits mediocre reduction of roof surface temperature that requires low initial cost, is easy to construct and does not require a mechanical system. A daily water temperature change of 5 °C is typical for an uncovered roof pond and a water depth of 0.3 m was recommended [4]. In a roof pond with 0.05 - 0.15 m water depth, roof surface temperature was reduced by 23 °C in comparison to a bare roof [5]. Most of the research results in previous studies of roof ponds were derived from field experiments in small- or full-scale models. Studies of thermal behavior in the uncovered roof pond have been inadequate in detail, so their application to date has been rather limited. In addition, determining an appropriate water depth in the roof pond in a hot and humid climate is needed to ascertain the applicability of a roof pond with a practical construction load.

The previous results of 0.3 m water depth for an uncovered roof pond in a hot and arid climate might not be suitable for a hot and humid climate. Due to the high relative humidity and mostly cloudy sky, less water evaporation and radiation are expected in a hot humid environment. At the water surface of an uncovered roof pond, water evaporation rates depend on parameters, ambient temperature (T_1); surface water temperature (T_w); characteristic length in the wind direction (L); wind velocity (v_{wind}) and relative humidity [6,7]. Due to the solar gain in the outdoor roof pond, the water evaporation process occurs at the water surface while the heat stored in water close to the surface causes a water temperature

increase. An increase in water depth reduces the penetration of accumulated heat into the pond's bottom. Furthermore, the increase of water volume help maintain room temperature against the variation of solar radiation and outdoor parameters. A conductive material has been recommended for roofs to maximize conduction heat transfer [8]. A thick concrete roof also acts as a heat storing mass that attenuates the heat storing effect in water [9]. Because there have been no investigations relating the role of roof supporting material in this field, a concrete roof in contact with a water pond bottom is simultaneously simulated with pond models in the present study.

This present study presents a simulation of temperature distribution in a 2 dimensional roof pond with water depths of 0.1 - 0.4 m on a concrete roof with a thickness of 0.1 m. The objectives are 1) to evaluate an appropriate water depth to prevent heat transfer under ambient conditions in a hot and humid climate, and 2) to propose a hybrid roof pond utilizing water flow. The boundary conditions involve a seasonal air temperature of 32.93 - 36.67 °C, an initial water temperature of 24.0 - 25.35 °C, and a room temperature of 24.0 °C in the daytime. During night time, water was expected to be cooled down via sky radiation under an air temperature of 25 °C. The average solar radiation absorbed at the water surface was kept at 638 W/m^2 and water evaporation rate was constant. The model presented here excludes the penetration of solar radiation to the pond bottom in order to ease the modeling procedures. Therefore, the results of temperature at the bottom of the pond are simulated according to constant boundary conditions. The simulation study include 2 functions of uncovered roof pond: roof pond with still water and roof pond with water flow. The simulation results were validated with the experimental results of the same roof pond depth, water and ambient temperatures obtained by Givoni [8]. Practically, a small water pump could be used for water circulation; that is, driving warm surface water away through the outlet and replacing the pond with cool water through the inlet. The fluid flow and temperature distribution in the water and the roof were obtained simultaneously by numerical simulation of the heat transfer model with the engineering software, COMSOL Multiphysics.

Formulation of the problem

The uncovered roof pond is exposed to outdoor and indoor parameters. **Figure 1** shows the roof pond system subjected to solar radiation (Q_{solar}), radiation heat loss to the sky (Q_{sky}), and convection heat and mass transfer ($Q_{convection}$ and $Q_{evaporation}$) at the water surface. As the roof pond system directly contacts the ceiling, there is conduction heat transfer between the pond bottom and the ceiling ($Q_{conduction}$). In this study the room temperature (T_{a2}) is assumed to be 24 °C and the roof pond walls are adiabatic. Due to the temperature difference between the top and the bottom of the roof pond, the buoyancy effect is also included in the model.

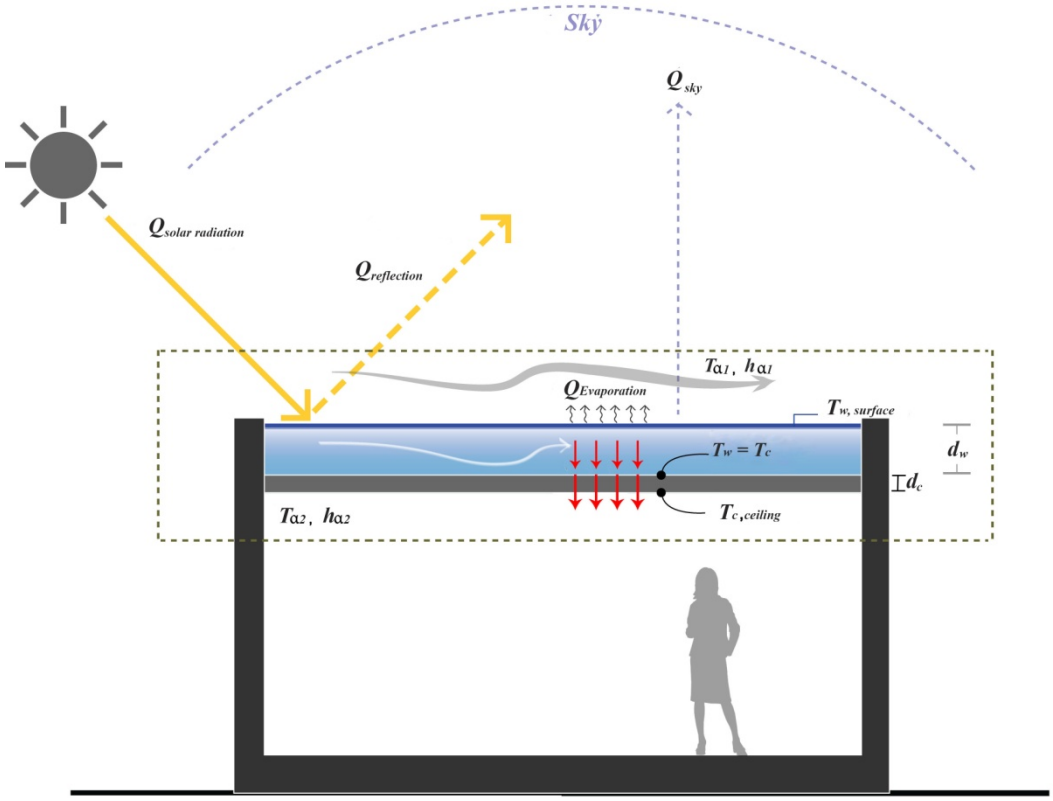

Figure 1 Uncovered roof pond subjected to outdoor and indoor parameters.

The studied parameters shown in **Table 1** include 5 water depths: 0.1, 0.2, 0.3 and 0.4 m varying with 2 roof pond lengths: 3.0 and 4.0 m under the ambient air ($T_{\alpha 1}$) and initial water temperatures (T_w) of 34 and 24 °C, respectively. The ambient air temperature of 34 °C is the average value of dry-bulb temperatures in the daytime during March - June 2013 [10]. The water temperature is derived from average wet-bulb temperatures during March - June 2013 [10]. The assumed room air temperature of 24 °C was equal to that of the initial water temperature. A solar intensity of 638 W/m^2 was the average value collected during 11 a.m. - 4 p.m. from [2]. The evaporation rate, e, of 6.75 W/m^2 was derived from $h_e(P_w - P_a)$, where h_e is the evaporative heat transfer coefficient (W/m^{2}Pa), and P_w and P_a are the water vapor partial pressure at the water and air temperatures (Pa), respectively [6]. In this study, h_e was calculated from $h_e = 0.036 + 0.025v_{wind}$ [11], the relative humidity in the air was 54.3 percent permitting the saturated water at 24 °C to evaporate at the specified ambient temperature of 34 °C. Designated as slow water flow, the inlet velocity in Model 2 was approximately constant at 0.1 m/s. The outdoor convection heat transfer coefficient ($h_{\alpha 1}$) was calculated from $h_{\alpha 1} = 2.8 + 3.0v_{wind}$, where v_{wind} was the wind speed, representing a calm environment [12]. For a calm environment, the differences between the outdoor ($h_{\alpha 1}$) and indoor ($h_{\alpha 2}$) convection heat transfer coefficients are neglected and $h_{\alpha 2}$ and $h_{\alpha 1}$ are assigned to be equal.

Table 1 Summary of studied parameters in the roof pond system.

Physical and environmental parameters	Values
Water depth (d_w, m)	0.1, 0.2, 0.3, 0.4
Concrete roof depth (d_c, m)	0.1
Roof pond length (L, m)	3.0, 4.0
Ambient temperature (T_{a1}, °C) [10]	34.0
Water temperature (T_w, °C) [10]	24.0
Room air temperature (T_{a2}, °C)	24.0
Solar intensity (G, W/m^2) [2]	638.0
Evaporation rate (e, W/m^2)	6.78
Wind speed (v_{wind}, m/s) [2]	0.73
Inlet velocity in Model 2 (V_{inlet}, m/s)	0.1
Outdoor& Indoor convection heat transfer coefficient (h_{a1}, W/m^{2}K)	5.00

The ambient air and water temperature representing summer, winter, and rainy seasons were investigated in the roof pond with a water depth of 0.2 m as shown in **Table 2**. The highest air temperatures collected from the weather station in Pathum Thani province in May, August and December 2013 were used here. The water temperatures were assumed to be less than the wet bulb temperature by 1 °C. The cool ambient temperature without solar radiation at night time is also included.

Table 2 Summary of studied parameters in the roof pond system with still water (Model 1).

Physical and environmental Parameters	Values
Water depth (m)	0.2
Roof pond length (m)	3.0
Ambient temperature (°C) [10]	
Summer, rainy, winter, night	36.67, 32.93, 33.67, 25.0
Initial water temperature (°C) [10]	
Summer, rainy, winter, night	24.82, 25.35, 23.67, 25.8

Table 3 Thermal properties of the roof pond [13].

	Water		Concrete
k_w (W/m°C)	0.607	k_c (W/m°C)	1.442
ε_w	0.95 - 0.96	ε_c	-
c_{pw} (J/kg°C)	4,180	c_{pc} (J/kg°C)	990
ρ_w (kg/m^3)	997	ρ_c (kg/m^3)	2400
d_w (m)	0.10 - 0.50	d_c (m)	0.10
υ_w (m^2/s)	1.457×10^{-7}	-	
β (1/K)	0.00332		

Methods and models

In this study a 2-dimensional model of an uncovered roof pond system has been developed. According to the control volume of an uncovered roof pond system in **Figure 1**, the 2-dimensional roof pond models shown in **Figures 2(a)** and **2(b)** were used in this study. These models comprise a water

layer and concrete layer with thermal properties as shown in **Table 3**. Model #1 of an uncovered roof pond with still water in **Figure 2(a)** consists of the opened boundary on the water surface, the continuous boundary of water in contact with the concrete roof, and the boundary of the concrete roof in contact with indoor air. Two walls close to the inlet and outlet of the roof pond models were assumed to be adiabatic. Under similar boundary conditions to that of the still water, **Figure 2(b)** shows model #2 of an uncovered roof pond with water flow including one inlet under the water and one outlet at the water surface.

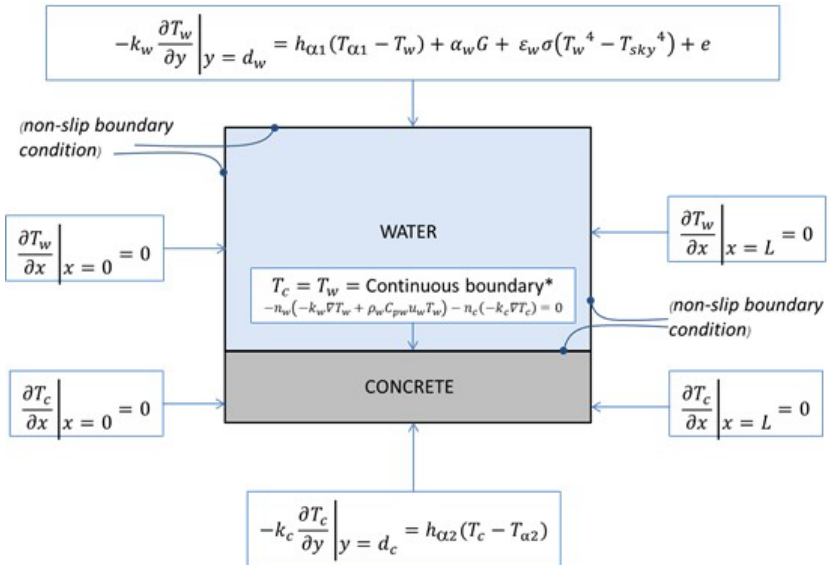

(a)

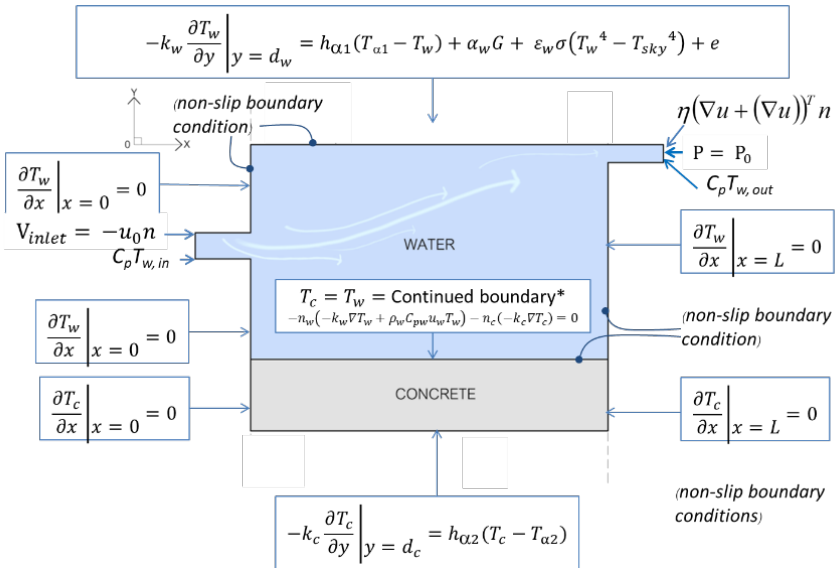

(b)

Figure 2 Boundary conditions for analysis of heat transfer and fluid flow in the roof pond system with (a) still water, Model 1, and (b) water flow, Model 2.

Heat transfer analysis of the roof pond system is modeled in 2 dimensions. To simplify the problem the following assumptions are made: 1) water and concrete are homogeneous materials with constant thermal properties, 2) there is no shadow casting on the water surface and thermal radiation was absorbed and emitted on the water surface uniformly, 3) there is no phase change in the water, 4) the pressure at the water surface equals atmospheric pressure, 5) heat loss due to evaporation at the water surface occurs with a constant rate [6], 6) buoyancy effects are modeled by Boussinesq's approximation and 7) the water is modeled as an incompressible Newtonian fluid. The governing equations of water flow in the water layer in the roof pond in **Figures 2(a)** and **2(b)** are Eqs. (1) - (3) as follows:

Continuity equation;

$$\frac{\partial u}{\partial x}+\frac{\partial v}{\partial y}=0 \tag{1}$$

Momentum equation;

$$\frac{\partial u}{\partial t}+u\frac{\partial u}{\partial x}+v\frac{\partial u}{\partial y}=-\frac{1}{\rho_w}\frac{\partial P}{\partial x}+\upsilon_w\left(\frac{\partial^2 u}{\partial x^2}+\frac{\partial^2 u}{\partial y^2}\right) \tag{2}$$

$$\frac{\partial v}{\partial t}+u\frac{\partial v}{\partial x}+v\frac{\partial v}{\partial y}=-\frac{1}{\rho_w}\frac{\partial P}{\partial y}+\upsilon_w\left(\frac{\partial^2 v}{\partial x^2}+\frac{\partial^2 v}{\partial y^2}\right)+g\beta\left(T_w-T_0\right) \tag{3}$$

The governing equation of heat transfer in the water layer in the roof pond consists of both conduction and natural convection as follows:

Energy equation for the water layer;

$$\rho_w C_w\frac{\partial T_w}{\partial t}-k_w\left(\frac{\partial^2 T_w}{\partial x^2}+\frac{\partial^2 T_w}{\partial y^2}\right)=-\rho_w C_w\left(u\frac{\partial T_w}{\partial x}+v\frac{\partial T_w}{\partial y}\right) \tag{4}$$

The governing equation of heat transfer in the concrete layer in **Figure 2** is the classical conduction heat transfer given in Eq. (5).
Energy equation for concrete layer;

$$\rho_c C_c\frac{\partial T_c}{\partial t}=k_c\left(\frac{\partial^2 T_c}{\partial x^2}+\frac{\partial^2 T_c}{\partial y^2}\right) \tag{5}$$

The heat transfer analysis is considered only in the roof pond system, the water layer and the concrete layer. The boundary conditions to solve governing equations are shown in **Figures 2(a)** and **2(b)** for the roof pond system with still water and with water flow, respectively. The water surface contacting with the environment is considered as convective, radiative and as having evaporative boundary conditions;

$$-k_w\left.\frac{\partial T_w}{\partial y}\right|_{y=d_w}=h_{\alpha 1}\left(T_w-T_{\alpha 1}\right)+\alpha_w G+\varepsilon_w\sigma\left(T_w^4-T_{sky}^4\right)+e \tag{6}$$

The bottom of the concrete layer or the ceiling surface is assumed to have a convective boundary condition;

$$-k_c \left.\frac{\partial T_c}{\partial y}\right|_{y=d_c} = h_{\alpha 2}\left(T_c - T_{\alpha 2}\right) \tag{7}$$

It is assumed that there is no resistant contact between the concrete and water at the bottom of the pond. Hence, the internal boundary is assumed to be a continuous boundary with T_w=T_c as follows;

$$-n_w\left(-k_w \nabla T_w + \rho_w C_{pw} u_w T_w\right) - n_c\left(-k_c \nabla T_c\right) = 0 \tag{8}$$

where n is the normal vector. In the roof pond system with still water (Model 1), the left and right sides of water are assumed to have adiabatic boundary conditions shown in **Figure 2**, where the heat transfer through this boundary is neglected;

$$\left.\frac{\partial T_w}{\partial x}\right|_{x=0} = 0, \quad \left.\frac{\partial T_w}{\partial x}\right|_{x=L} = 0 \tag{9}$$

Similarly, the boundary conditions of the left and right sides of the concrete are assumed to be adiabatic as follows;

$$\left.\frac{\partial T_c}{\partial x}\right|_{x=0} = 0, \quad \left.\frac{\partial T_c}{\partial x}\right|_{x=L} = 0 \tag{10}$$

In the roof pond system with water flow (Model 2) shown in **Figure 2(b)**, the boundary conditions for heat transfer analysis are similar to those of Model 1 except for the inlet and outlet on the left and right sides of the water layer. According to the first law of thermodynamics, under slight differences in water temperature at the inlet and outlet, the internal energy is assumed to be $C_{pw}T_{w,\,in} \approx C_{pw}T_{w,\,out}$.

The internal surfaces in the roof pond system shown in **Figure 2** are specified with no slip boundary conditions for solving the momentum equation. In the roof pond system with water flow (Model 2) shown in **Figure 2(b)**, the boundary conditions for fluid flow analysis is at a constant inlet velocity, u_o, of 0.1 m/s flowing normal to the cross sectional inflow area.

$$u = -u_0 n \tag{11}$$

At the outlet, the pressure is considered with no viscous stress. This boundary condition is specified as follows;

$$P = P_0 \text{ and } \eta\left(\nabla u + (\nabla u)\right)^T n \tag{12}$$

Calculation procedures

The finite element model is discretized using triangular elements with Lagrange quadratic shape functions. The fine mesh is specified in the water layer and closed to the boundaries. This study provides a variable mesh method for solving the problem as shown in **Figure 3**. The set of governing equations consisting of the energy equation, momentum transport, continuity equation, and their related boundary conditions were solved via COMSOLTM multiphysics. A convergence test was conducted to identify the appropriate number of meshes required.

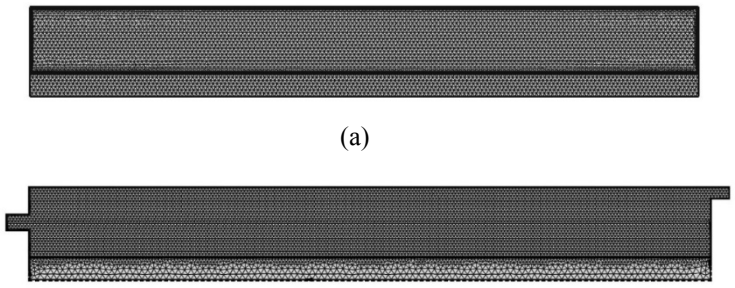

(a)

(b)

Figure 3 (a) A 2D finite element mesh of the uncovered roof pond (a) Model 1 and (b) Model 2.

The simulation results of water temperature collected from coordinate x = 1.5 m and y = 0.25 m in Model 1 with a water depth of 0.3 m and mesh number variation from 1500 to 150,000 are shown in **Figure 4**. This convergence test shows that the number of meshes where the solution is independent of mesh density is around 25,000. This convergence test leads to mesh numbers within the studied domain of approximately 21,600 - 25,000 elements. In the verification part, Model 1 with a water depth of 0.3 m used fine meshes of 50,000 elements.

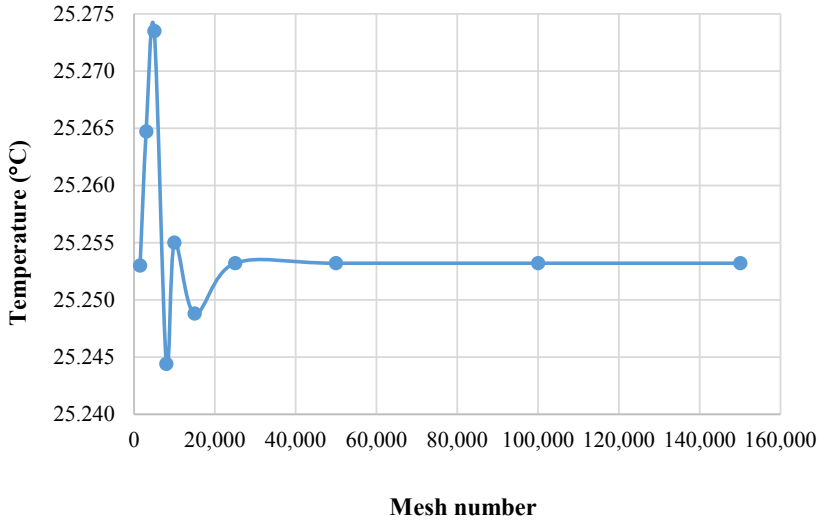

Figure 4 Mesh independent test of the 2D model.

Results and discussion

Verification of the model

In order to verify the accuracy of the present numerical models, the simulated results from this study are validated against the experimental results obtained by Givoni [8]. The validation case assumes an identical roof pond geometry with a water depth of 0.3 m, an ambient temperature of 40 °C, an initial water temperature of 19 °C and a room air temperature of 35 °C. During 6 h of operation, the simulation results show good agreement between water and ceiling temperatures (see **Figure 5**). This close comparison is reassuring regarding the accuracy of the current numerical model.

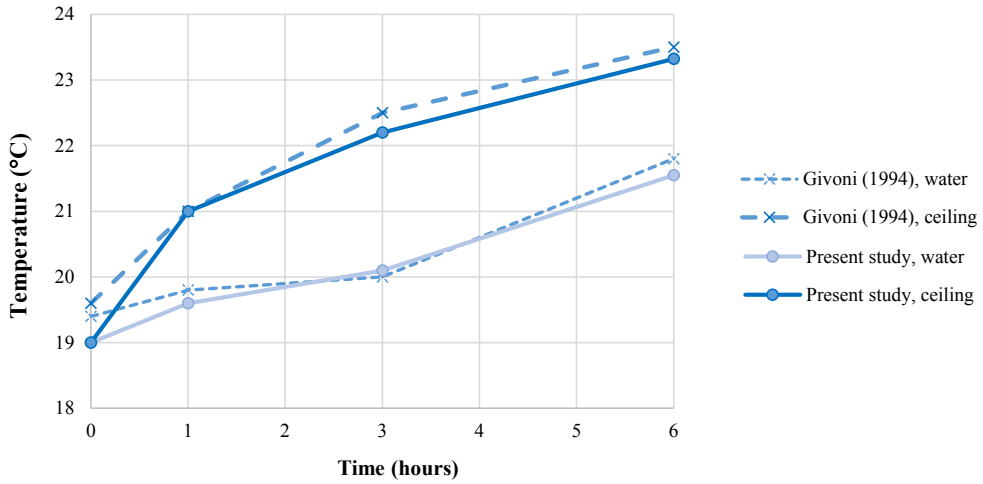

Figure 5 Comparison of the calculated water and ceiling temperature alteration over 6 h to the results obtained by Givoni [8].

Temperature distribution in roof pond with still water

The effects of water depths

In this section, the effect of water depths on the temperature distribution is investigated. **Figure 6** shows the simulation results of temperature distribution in the roof pond with still water for 6 h. The temperature stratification in the water layer clearly shows that the buoyancy effect keeps warm water remaining in the upper part and cool water staying in the lower part of the pond. In the case with a water depth of 0.1 m, it is found that heat on the water surface penetrates to the pond bottom. Starting from a water depth of 0.2 up to 0.4 m, water temperatures in the pond are equal to that of the concrete roof. The water depth of 0.2 up to 0.4 m performs as thick insulators to prevent heat transfer. **Figure 7** displays the results of the temperature profile in the roof pond system with a water depth of 0.1 - 0.4 m.

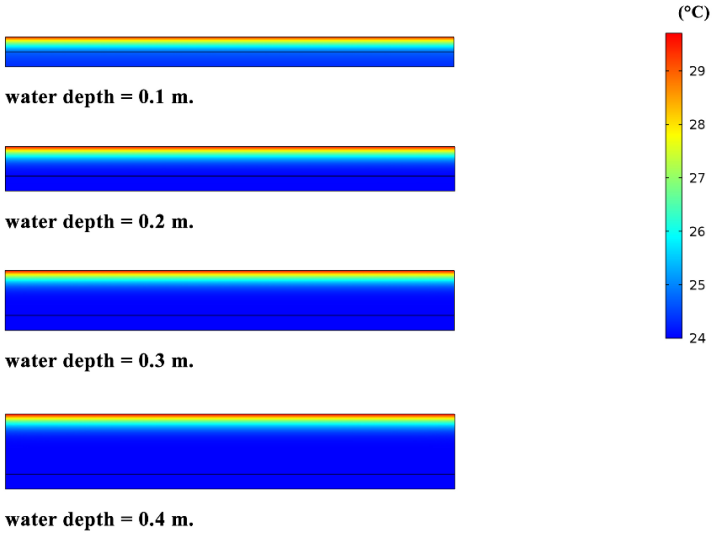

Figure 6 Simulation results of temperature distribution in the roof pond with still water for 6 h.

Figure 7 shows a temperature of around 29.7 °C at the water surface, increasing by 5.7 °C from 24.0 °C from the initial value. At the pond bottom, the water temperature is 24.9 °C in the case with a water depth of 0.1 m and the temperatures are about 24.0 °C for other cases which are similar to the initial value. Therefore, the minimum water depth of 0.2 m is sufficient to avoid heat transfer from the roof pond into the room under it. Considering the ceiling temperature under the roof pond with a water depth of 0.1 m, the ceiling temperature increase is minimal. That is, it increased from 24.0 to 24.38 °C with respect to the designated boundary conditions and assumptions.

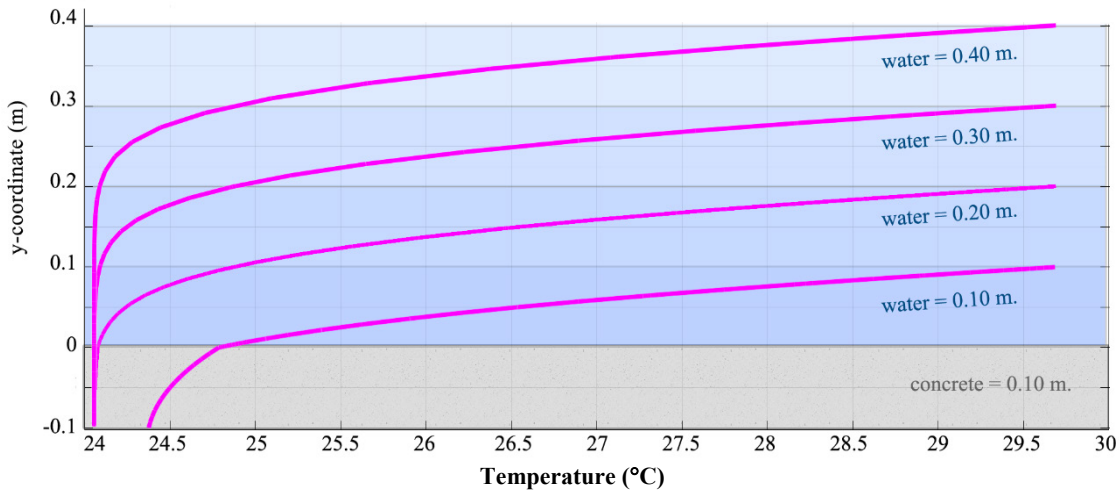

Figure 7 Temperature profiles in the roof pond system with water depths between 0.1 - 0.4 m.

The effect of roof pond length

The simulation results show no difference in temperature distribution in the increase of roof pond length from 3.0 to 4.0 m. Without water flow, the distribution of temperatures from the water surface to the concrete ceiling are similar as shown in **Figure 8**.

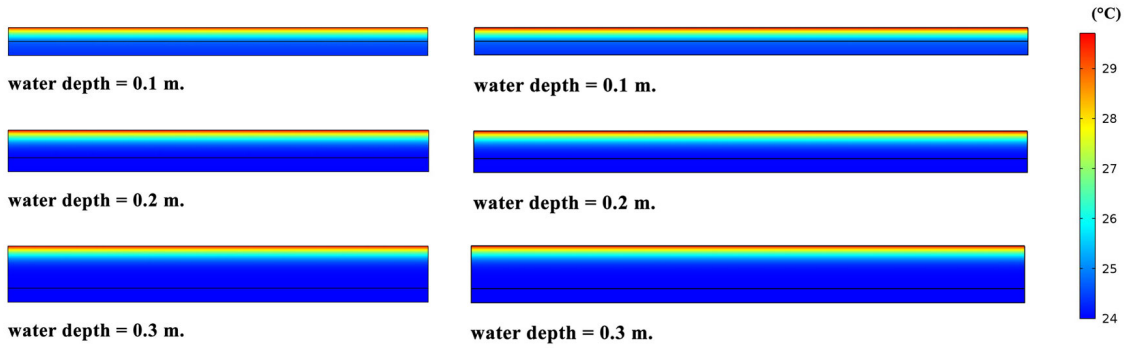

(a) (b)

Figure 8 Temperature distribution in the roof pond with still water with (a) roof span = 3.0 m and (b) roof span = 4 m.

The effect of ambient air and water temperatures due to seasonal and nighttime changes

In this section the water depth of 0.2 m with variation of ambient temperatures and water temperatures representing summer, rainy and winter seasons as well as night time in Thailand were simulated. The maximum ambient temperatures were collected from a weather station in Pathum Thani province (see **Table 3**). The simulation results of the 6 operation hours in the daytime (1 p.m. - 7 p.m.) of summer, rainy and winter seasons and 9 h (8 p.m. - 5 a.m.) in the night time of summer are depicted in **Figure 9**. The initial water temperatures ranked from high values to low values were 25.8 °C (night time in summer), 25.35 °C (daytime in rainy), 24.82 °C (daytime in summer), and 23.67 °C (daytime in winter), respectively. **Figure 8** shows the temperatures at the pond bottom and the ceiling resemble the initial water temperature. This implies that water temperature completely dominates the ambient temperature and it also directly affects ceiling temperature. In the summer night time, summer daytime and rainy seasons, water temperature is higher than the room air temperature that would increase the cooling load. Therefore, the control of water temperature during the summer and rainy season is required. The roof pond with water flow presented in the next section is a viable method in controlling water temperature.

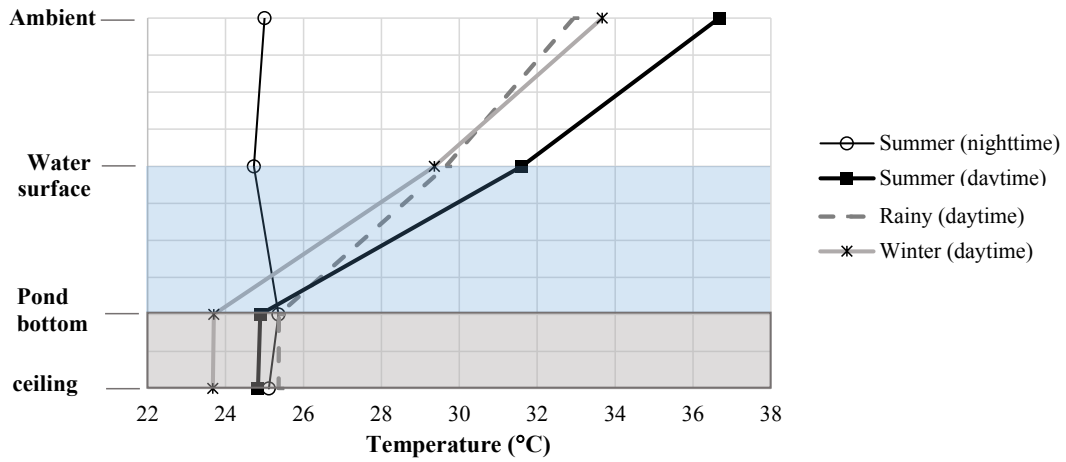

Figure 9 Simulation results of roof pond with still water under 4 ambient conditions (night time of summer, daytimes of winter, rainy and summer).

Temperature distribution in the roof pond with water flow

The effect of water depths

Under the ambient temperature of 34 °C and water temperature equal to a room air temperature of 24 °C, the simulation results of the roof pond with water flow show solar heat and convection heat transfer from the water surface downward through its depth. In this study water flows along the pond span, with the natural and forced convection processes occur simultaneously. Therefore, the temperature distribution in the pond is governed by the mixed convection process. **Figure 10(a)** shows the simulation results of temperature distribution in the roof pond with water flow varying in depths across 6 operation hours.

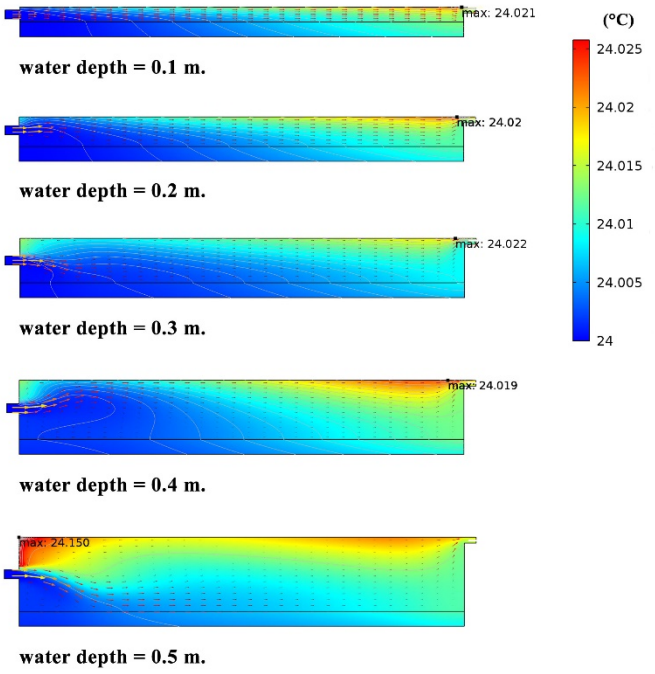

(a)

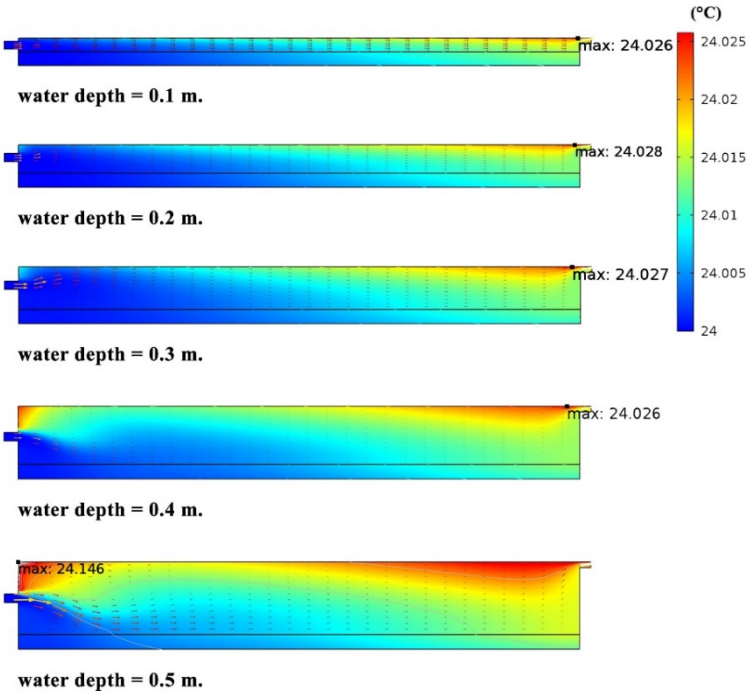

(b)

Figure 10 Temperature distribution and velocity vectors in the roof pond with water flow (a) roof span = 3.0 m and (b) roof span = 4 m.

The inflow velocity is 0.1 m/s and the height of the inlet and outlet are 0.05 m. The inlets of the roof pond with water depths between 0.1 - 0.4 m are close to the water surface. **Figure 10** shows that water flow from the inlet and exit at the outlet, removing warm water at the pond surface out of the pond. As seen in **Figure 10(a)**, there are only minor temperature differences in the roof pond with water flow. However, temperature gradients are visible in both the water pond and the concrete roof. The velocity vectors illustrated in **Figure 10(a)** show a higher water velocity at the high region in comparison to that of the low region. The mixed convection and the temperature difference produce a vortex of inflow water beneath the inlet which reduces water and concrete temperatures. At the outlet, water temperature increases because the pressure difference creates water recirculation in that area. As shown in **Figure 10(a)**, the increase of water depth and the deep immerged inlet bring about water recirculation in the roof pond and the roof temperature tends to increase.

The effect of roof pond lengths

Figure 10(b) indicates that the roof pond length affects velocity and temperature distributions. The results show that the longer the flow distance, the lower the flow velocity is approaching the outlet. In turn, this intensifies water recirculation and temperature gradients. However, there is no significant effect of water depth or water flow distance on the increase of temperature in this study. Water temperature is comparable to the inlet temperature of 24 °C.

The uncovered roof pond with water flow is thermally efficient, but it would demand high operation costs. A hybrid roof pond, which stores water during the daytime and permits water flow in the morning, is an alternative and viable roof pond system. The simulation result of the roof pond with a water temperature of 25.5 °C that is replaced by the circulation water with a temperature of 24 °C is shown in **Figure 11**. Due to a satisfactory prevention of heat transfer at minimum water depth, the roof pond of 0.2 m water depth is chosen to illustrate the hybrid roof pond system here. As indicated in **Figure 11**, water entering the roof pond with a depth of 0.2 m and a span of 3 m can reduce temperatures within 5 min. The roof pond with still water of 24 °C is then used to absorb heat during the daytime. The removed warm water is retreated to reuse in the roof pond for the next circulation.

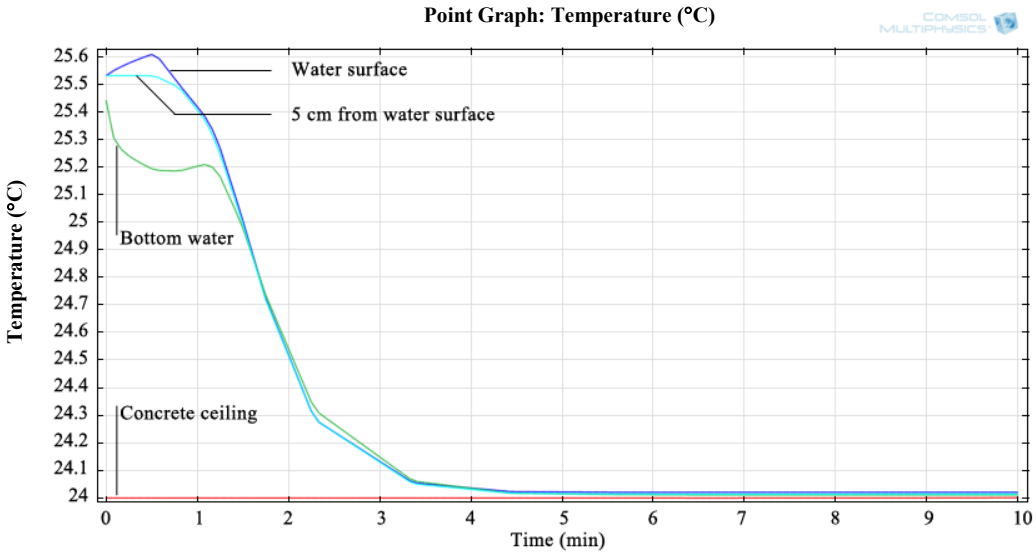

Figure 11 Temperature reduction in the roof pond with a water depth of 0.2 m and a roof span of 3 m by using a water circulation process.

Conclusions

The effect of water depth, pond span, air and water temperatures on the temperature distribution in the uncovered roof pond system have been investigated. The temperature distribution in water and the concrete roof during exposure to air and water temperature in the night time, summer, rainy season and winter were obtained by numerically simulating the heat transfer model.

We found that temperature distribution in the water was directly influenced by the water's initial temperature and water depth. The increase of ambient air temperature gives rise to higher water surface temperatures which are compensated by water latent heat loss. Water depths greater than 0.2 m show minimal effects on concrete roof and ceiling temperatures. A water depth of 0.2 m with an initial temperature of less than or equal to room temperature is recommended to resist ambient fluctuation in hot and humid climates. In the roof pond with still water, the water temperature tends to increase in summer and rainy seasons and this brings about a warm ceiling. Compared to the roof pond with still water, the roof pond with water flow performs better in keeping constant water and concrete temperatures. The water temperature at the surface of the roof pond with still water is higher than that of the roof pond with water flow by 4 °C. In order to keep the water temperature at the pond bottom constant, removing warm water from the pond and replacing it with cool water by water circulation is suggested once a day.

Acknowledgements

The authors gratefully acknowledge the Thailand Research Fund (under the TRF contract No. RTA5680007) and the National Research University Project of Thailand Office of Higher Education Commission. This research was financially supported by Thammasat University Research Fund under the TU Research Scholar, Contract No. 61/2557.

References

[1] M Srivanich and K Hokao. Thermal infrared remote sensing for urban climate environmental studies: an application for the city of Bangkok. *J. Architect. Res. Stud.* 2012; **9**, 83-100.
[2] S Chungloo and B Limmeechokchai. Application of passive cooling systems in the hot and humid climate: the case study of solar chimney and wetted roof in Thailand. *Build. Environ*. 2007; **42**, 3341-51.
[3] A Spanaki, T Tsoutsos and D Kolokotsa. On the selection and design of the roof pond variant for passive cooling purposes. *Renew. Sust. Energ. Rev*. 2011; **15**, 3523-33.
[4] S Yannas, E Erell and JL Molina. *Roof Cooling Technique: A Design Handbook.* Earth-Scan, James & James, UK, 2006.
[5] GN Tiwari, A Kumar and MS Sodha. A review-cooling by water evaporation over roof. *Energ. Convers. Manag.* 1982; **22**, 143-53.
[6] E Satori. A critical review on equations employed for the calculation of the evaporation rate from water surfaces. *Sol. Energ.* 2000; **68**, 77-89.
[7] MM Shah. Improved method for calculating evaporation from indoor water pools. *Energ. Build*. 2012; **49**: 306-309.
[8] B Givoni. *Passive and Low energy Cooling of Building*. John Wiley & Sons, New York, 1994.
[9] S Raessi and M Taheri. Skytherm: An approach to year-round thermal energy sufficient houses. *Renew. Energ.* 2000; **19**: 527-43.
[10] Thai Meteorological Department. Weather Data at Pathumthani Meteorological Station. 2013.
[11] W McMillan. Heat dispersal-Lake Trawsfynydd cooling studies. *In*: Proceedings of the Freshwater Biology and Electrical Power Generation. Leatherhead, UK, 1971, p. 41-80.
[12] JA Duffie and WA Beckman. *Solar Engineering of Thermal Process.* John Wiley & Sons, New York, 1991.
[13] Y Cengel. *Heat Transfer*. McGraw-Hill, Singapore, 2004.